designs

MDPI

Article

Metal-Doped Nanostructured Carbonic Materials and Their H_2 Adsorption—An Experimental Approach

Radu Mirea [1,*], Gimi A. Rimbu [2,*] and Mihai Iordoc [2]

[1] Romanian Research and Development Institute for Gas Turbines—COMOTI, 220D Iuliu Maniu Boulevard, 061126 Bucharest, Romania
[2] National Institute for Research and Development in Electrical Engineering, ICPE-CA, 313 Splaiul Unirii, 030138 Bucharest, Romania
* Correspondence: radu.mirea@comoti.ro (R.M.); gimi.rimbu@icpe-ca.ro (G.A.R.); Tel: +40-724-977-646 (R.M.); +40-721-595-990 (G.A.R.)

Abstract: Experimental assessment of the hydrogen (H_2)-adsorption capacities of metal-doped carbon nanostructured materials were investigated in this study. Given their intrinsic characteristics, nanostructured carbonic materials show great potential for different applications that require H_2, one such being their use as hydrogen carriers in the automotive sector. The current paper considers two types of carbonic substrates (carbon nanotubes and polyaniline) functionalized and doped with platinic metals: Pt, Ru and Ir. The H_2-adsorption capacities of the materials were assessed at 293 K and at relatively low pressures (10, 20 and 30 bar). Thus, nanostructured polyaniline (p-$C_6H_5NH_2$) and multi-walled carbon nanotubes (MW-CNTs) were subject to noble-metal doping in order to assess their physical H_2-adsorption capacities. The two types of substrates have different structures and characteristics, one being a "synthetic metal" and the other an amorphous carbon substrate. The metals used for doping were Platinum (Pt), Iridium (Ir) and Ruthenium (Ru), and the doping procedure consisted of chemical reaction between the metals' salts and the carbonic substrate after the latter's physical activation. Physical H_2-adsorption capacity was determined with equipment designed to measure porous materials' adsorption capacities at pressures ranging from 1 to 200 bar. The obtained results showed an increase inH_2-adsorption capacity of 293% from 10 to 30 bar for Ru, 270% for Ir and 256% for Pt doping in the case of the MW-CNTs, and 296% for Ru, 282% for Ir and 251% for Pt from 10 to 30 bar in the case of p-$C_6H_5NH_2$. As the main conclusion, even though Pt is known to be the main metal used in reactions involving H_2, Ru and Ir showed better potential for this application, namely, as hydrogen-carrier materials for use in the automotive sector.

Keywords: adsorption capacity; polyaniline; carbon nanotubes; doping

Citation: Mirea, R.; Rimbu, G.A; Iordoc, M. Metal-Doped Nanostructured Carbonic Materials and Their H_2 Adsorption—An Experimental Approach. *Designs* **2022**, *6*, 86. https://doi.org/10.3390/designs6050086

Academic Editor: Yen-Linh Thi Ngo

Received: 23 August 2022
Accepted: 26 September 2022
Published: 28 September 2022

1. Introduction

Carbonic materials are a unique type of material, since they display a rather interesting array of characteristics: increased surface area, microporosity, chemical stability, etc. [1]. However, they are not the best materials to be used for H_2 storage due to the fact that, despite their high porosities, only a fraction of these pores are in the diameter range suitable for their interaction with H_2 molecules and the storage of H_2 within their inner structures, especially at moderate pressures and room temperatures [2]. Theoretical calculations made by Ulrich [3] determined that, in specific configurations, MW-CNTs can provide a leakage-free material up to 10,000 bar. Nevertheless, this value is a theoretical one, and, as the authors of [1,4–6] have demonstrated, at moderate pressures (up to 5 bar) 6.5 wt.% of H_2 adsorption can be achieved. Moreover, the US-EERE (American Office of Energy Efficiency and Renewable Energy) has set a bold target of 4.5 wt.% of H_2 at 1 bar [7].

Current research has shown that carbonic materials' properties in terms of H_2-storage capacity can be tailored towards a significant increase by doping them with transitional metals or even metal alloys. It has been demonstrated that MW-CNTs doped with TiAlO can absorb up to 6 wt.% of H_2 at temperatures ranging from 573 to 623 K [4,6]. In the automotive sector, such high temperatures are difficult to obtain and maintain, so the study aimed to assess the H_2-adsorption capacities of the developed materials at room temperatures but at pressures comparable to the ones within LPG tanks currently mounted on vehicles. Thus, the testing pressures used were between 10 and 30 bar, given the fact that H_2 is actually adsorbed within the carbonic material.

The adsorption phenomenon takes place when the surface of the material is modified in order to create functional groups to embed the metal doping [8]. Surface enhancement may be achieved by several techniques [9,10], but the one used in the current study was high-frequency ultrasound [4]. The use of ultrasound was necessary to induce fractures within the materials' inner structures in order to create the functional areas mentioned above. Since Pt is the doping metal usually used in reactions involving H_2, it is understandable that it was chosen for the carbon-based substrates [11]. At the same time, Pt may be an expensive material, so cheaper alternatives were selected: Ir and Ru. All three of them are known for being very reactive and suitable for use in improving the H_2-adsorption capacity of a substrate, but their characteristics in terms of electronegativity and electron affinity vary. The most reactive of them is Pt, having an electronegativity of 2.28 and an electron affinity of 205.3 kJ/mole, while Ir has an electronegativity of 2.2 and an electron affinity of 151 kJ/mole and Ru has an electronegativity of 2.2 and an electron affinity of 101.3 kJ/mole.

The substrate [12] doping was performed by chemical means—the reduction of metal salts in the presence of acids, after their functionalization by using high-frequency ultrasound—since it presents one great advantage compared with physical doping procedures: reproducibility. Metal particles deposited on the substrate enhance H_2 adsorption, but their most important role is that they "send" the dissociated hydrogen molecules and spill them over to the carbonic substrate [4]. A modified porosity of the substrate can absorb large quantities of H_2, mainly due to the attractive potential of pore walls. In ref. [8], the atoms of the adsorbed gas migrated away from the metallic dopant deep inside the substrate material. Nowadays, researchers are focused on fully understanding the spill-over process [13], but it is widely accepted that, in order to obtain a notable result in terms of H_2-adsorption-capacity increase, the main condition regarding the substrate is to let the hydrogen atoms "travel" away from the metal [1].

A variety of substrates are currently under research, as presented in [14], starting from quite simple ones, such as MCM-41 mesoporous silica doped with the most regular metals, such as Fe, Ni, Ti, CO and Mg, and with rather modest results in terms of H_2-storage capacities ranging from 0.003 to 0.012 wt.% at 10 bar and 77 K [15]. Some research is focused on more "sophisticated" substrates, as presented in [16], where organic complexes made of benzene based complexes where boron atoms are used as substitutes for carbon atoms within benzene molecule and Li, Ca and Be were used as metals for doping, the newly obtained complexes, show results ranging from 2.26 wt.% for the Be-doped substrate to 6.82 wt.% for the Li- and 7.54 wt.% for the Ca-doped substrates.

The results published by Hussain et al. [17] for a 2D boron–graphdiyne nanosheet as a substrate doped simultaneously with four metal atoms (Li, Na, K and Ca) are impressive; the authors managed to obtain up to 14.29 wt.% of H_2 at 1 bar and 100 K.

Moreover, papers such as Divyia et al.'s [18] have tackled the obtainment of carbon-based substrates, namely, hydrogen-exfoliated graphene sheets doped with platinum for hydrogen adsorption. Their results showed a very promising start by obtaining a storage capacity of a maximum 1.4 wt.% at 25°C and 3 MPa (30 bar).

High-surface-area carbon materials doped with Pt, Ru and Ni have been studied by Wang et al. in [19]. They discovered that when doping templated and super-activated

(AX-21) carbon, the H_2-storage capacities varied as follows: Ru/C > Pt/C > Ni/C, but the maximum storage capacity obtained was 1.56 wt.% at 298 K and 103 bar.

A very deep insight related to the progress reported on the development of materials used for hydrogen storage from 2013 to 2018 [20] has shown that high gravimetric percentages of adsorbed H_2 of up to 15 wt.% can be achieved at 77 K and 50 bar. In this paper [20], the authors agreed that future fundamental studies within this field would focus on nanostructured materials as supports.

Having in mind the above-mentioned aspects, the current paper tackles two types of carbonic substrates (carbon nanotubes and polyaniline) functionalized and doped with *platinic metals*: Pt, Ru and Ir. Their H_2-adsorption capacities were assessed at 293 K and at relatively low pressures (10, 20 and 30 bar). As compared with the results reported in the literature, the ones obtained for the above-mentioned materials are much more promising, thus representing added value in the field of nanostructured carbonic materials for use in hydrogen adsorption.

2. Materials and Methods

In order to carry out the research work reported in this paper, MW-CNTs were purchased from the market but p-$C_6H_5NH_2$ was prepared in the lab. Both substrates were doped with metals using the chemical doping method of metal salt reduction with formic acid. All the reactants used in this paper were purchased from Sigma-Aldrich, Darmstadt, Germany, Europe.

2.1. Method for Preparing Polyaniline p-$C_6H_5NH_2$

A quantity of 3.82 g of 0.2 M aniline sulphate ($C_{12}H_{16}N_2O_4S$) was chemically oxidized with 5.71 g of 0.2 M ammonium peroxy-disulphate ($(NH_4)_2S_2O_8$), as in [9–11]. Each of the 99.99%-purity reactants were dissolved in separate Berzelius beakers in 50 mL of H_2SO_4 at a concentration of 0.2 M at room temperature under continuous stirring in order to allow polymerization reactions to occur. After 2.5 h, the obtained mixtures were filtered and washed with H_2SO_4 in order to eliminate all the by-products. In addition, the precipitates were washed with $(CH_3)_2CO$ to more thoroughly clean the precipitates of the by-products. The obtained result was a "synthetic metal": polyaniline sulphate (p-C_6H_5-NH-HSO_4).

2.2. Method for Preparing Metal-Doped Polyaniline p-$C_6H_5NH_2$

The procedure was similar to that performed for the 3 metal salts used for the substrate and was as follows:

A quantity of 0.5 g of the obtained "synthetic metal", p-C_6H_5-NH-HSO_4, was dispersed in deionized water, and a 70 kHz high-frequency ultrasound cannon was used to induce fractures within the p-$C_6H_5NH_2$'s internal structure, allowing the metal salt grains to adhere to the substrate. It was calculated that this frequency was sufficient to fracture the inner part of the substrate.

Then, 1 g of $NaHCO_3$ was added to the solution and brought to boil for 0.5 h.

In a separate Berzelius beaker, equal quantities (0.5 g) of the metal salts—H_2PtCl_6, $RuCl_3 \cdot H_2O$ and $IrCl_3$—were dissolved in 50 mL of deionized water underboiling and continuous stirring. After that, 3 cm^3 of formic acid was mixed with 25 cm^3 of purified water and poured over the dissolved salt. This mixture was kept at 80 °C for 0.5 h and then poured over the above-described functionalized p-$C_6H_5NH_2$.

This final mixture was kept at 80 °C for 1 h under the influence of the ultrasound cannon and then vacuum-filtered and washed with deionized water until its pH = 7.

The precipitate was dried at 100 °C for 3 h and then ground to a grain size of 0.5 mm.

2.3. Method for Preparing the Metal-Doped MW-CNTs

As in the case of p-$C_6H_5NH_2$, the same procedure was applied for all the metals, as follows:

Equal quantities (0.25 g) of the metal salts—H_2PtCl_6, $RuCl_3 \cdot H_2O$ and $IrCl_3$—and MW-CNTs were mixed with 50 cm^3 of deionized water and heated to 80 °C under continuous stirring. The same high-frequency ultrasound cannon was used to induce fractures within the CNT structures. Then, 5 cm^3 of formic acid was added to each mixture and this was brought to boil and kept for 1 h. After that, the solution was filtered, and the solid part was washed using deionized water until its pH = 7. Then, it was dried for 3 h at 100 °C.

The resultant solid did not need to be ground to obtain a fine granulated product.

The MW-CNTs used were TNMCN7s, produced by Chengdu Organic Chemicals Co. Ltd. Chinese Academy of Sciences, Chengdu, China, and had the following properties [12]:

OD (outer diameter): 30–80 nm;
Purity: >98 wt.%;
N content: >2.5 wt.%;
Length: 10–30 μm;
SSA (specific surface area): >30 m^2/g.

2.4. Methods for Substrate Characterization

2.4.1. X-ray Diffraction

A D8 Advanced XRD instrument, produced by Brucker, that uses wide-angle X-ray scattering was employed. Its main characteristics are: Cu anode (λ = 1.54059), Goebel mirror and 1D LynxEye secondary detector optics. The plots were drafted at a 0.04° angle increment and a scanning speed of 1 s/step. The sample was polished with a 5 μm soapstone and then put in the equipment for analysis.

2.4.2. N_2 Adsorption Experiments

The Autosorb-1, provided by Quanta chrome Europe, was used to measure the samples' and micropores' surfaces. The method used was physical adsorption/desorption of nitrogen gas on the materials' and open pores' surfaces. The working pressure ranged from 0.001 to 1 bar and allowed the determination of the following: BET surface micropore properties, including surface area.

2.5. Method for the Adsorption-Capacity Measurement of the Doped Carbonic Materials

The method used to determine the H_2-adsorption capacities of the doped materials was the physical adsorption method. The method relies on measuring the amount of gas stored within a porous material at different set pressures. The equipment used was a PCT-PRO User, provided by Setaram, Lyon, France. The equipment allows gas (H_2 included)-adsorption-capacity measurements at pressures ranging from 1 to 200 bar (the standard pressure of a 50-litre gas tank provided by Linde Romania). Thus, 1 g of sample was put in a high-pressure container and gaseous hydrogen was introduced into the container until the set pressure was reached and then the amount of gas adsorbed by the material was measured. The results are given in wt.% vs. pressure at room temperature.

3. Results and Discussion

All the samples were structurally and functionally tested as follows: from the *structural* point of view, XRD was used to determine N_2 adsorption for total and micropore surface areas, and from the *functional* point of view, H_2-adsorption capacity was measured.

3.1. XRD Assessment

XRD plots were drafted in order to emphasize the presence of metals within the structures of the carbonic materials. The method relies on the analysis of the crystalline phase embedded in a sample.

As can be observed, Figure 1a shows the crystalline structure of the graphite enclosed within the nanotubes (~2Θ = 26). Due to its sp^3 hybridization, the graphite peaks stand on their own within the amorphous structures of the nanotubes; it is well known that sp^3 hybridization can be observed using X-rays due to its similitude to a crystalline structure. The situation changes after the doping procedure, when metal crystalline forms started to appear within the materials' structures. Thus, Figure 1b shows a well-defined crystalline structure of Pt, the peak of which is considerably larger than the graphite's. It is to be mentioned that Pt has a face-centred crystalline structure, as does Ir, while Ru has a hexagonal structure. Figure 1c,d also show metal crystals embedded within the carbonic substrate, but their peak dimensions are lower than graphite's. One possible explanation is the electronegativity of the metals. Thus, the proposed chemical reduction of their salts does not provide results similar to those for Pt. So, the next step in this research may be the use of a stronger acid than formic acid.

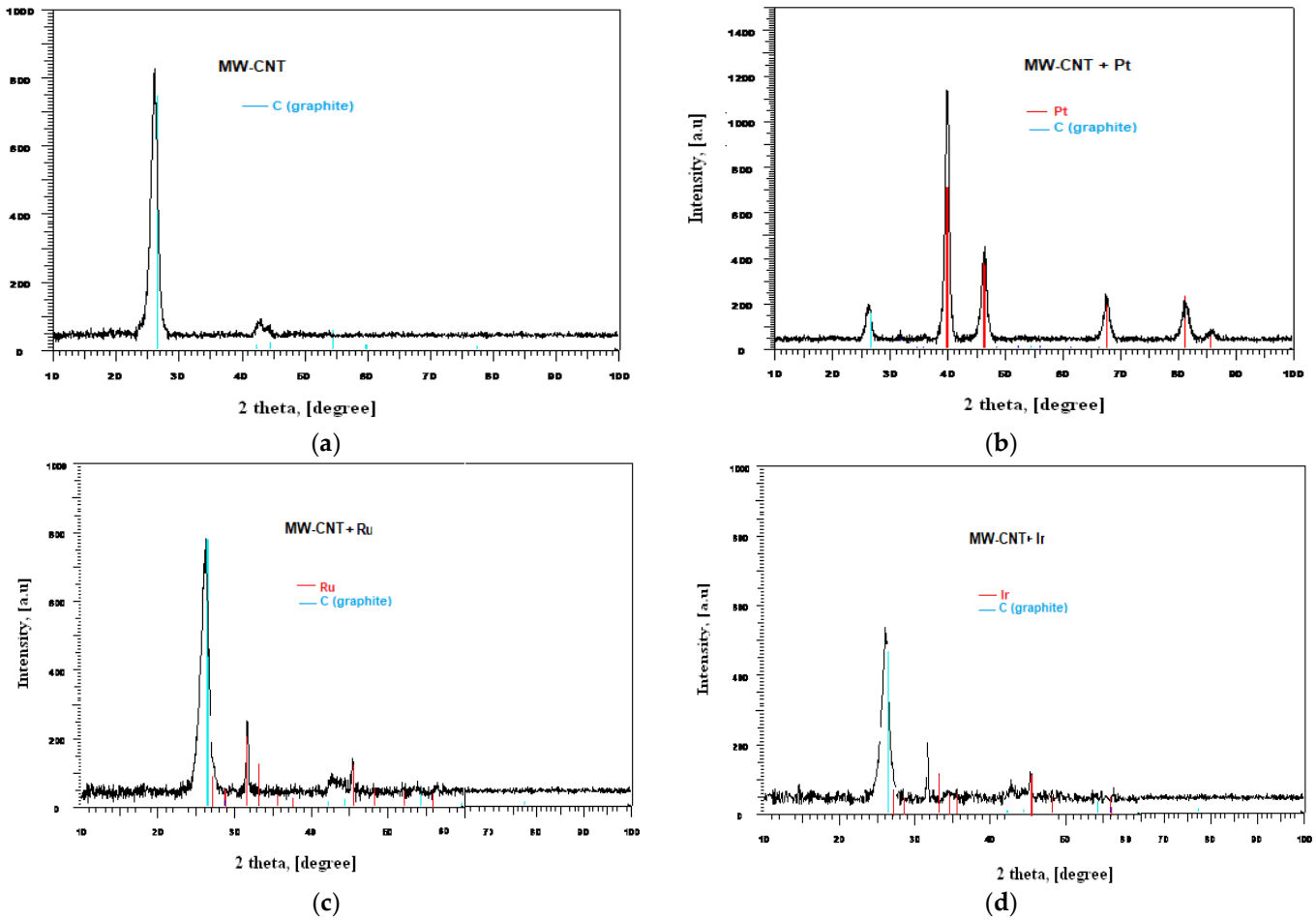

Figure 1. X-Ray plots for (**a**) MW-CNTs, (**b**) MW-CNTs + Pt, (**c**) MW-CNTs + Ru, (**d**) MW-CNTs + Ir.

Figure 2 shows the presence of the metal crystalline forms embedded in the substrates. Unlike MW-CNTs, p-$C_6H_5NH_2$ does not have sp^3 hybridization; therefore, its structure is entirely amorphous, as can be observed in Figure 2a. The peak sizes in the case of p-$C_6H_5NH_2$ doping are similar to those of the MW-CNTs in terms of size and shape, Pt being the best-represented.

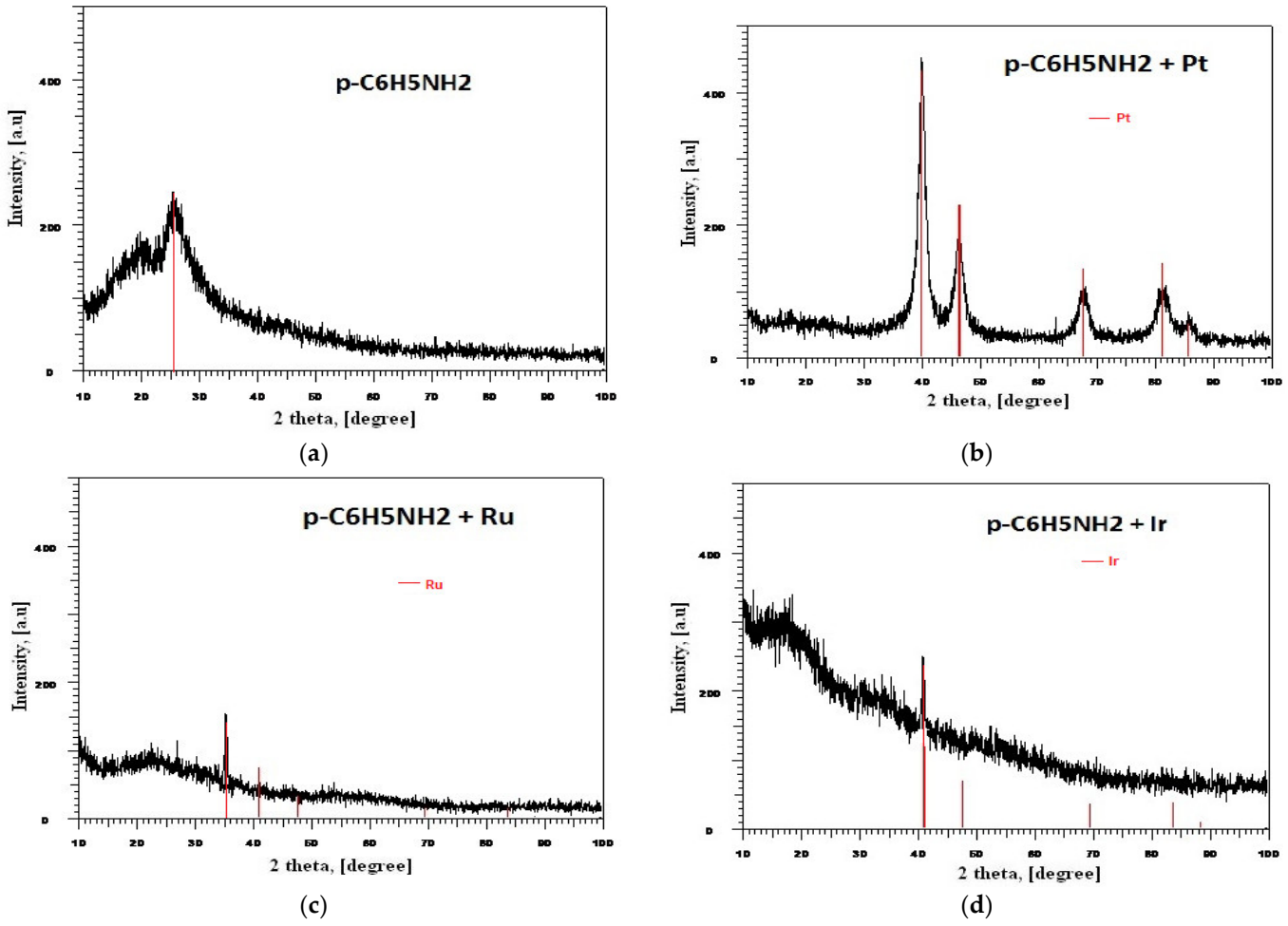

Figure 2. X-Ray plots for (**a**) p-$C_6H_5NH_2$, (**b**) p-$C_6H_5NH_2$ + Pt, (**c**) p-$C_6H_5NH_2$ + Ru, (**d**) p-$C_6H_5NH_2$ + Ir.

3.2. N_2-Adsorption Experiments

By determining the total amount of gas adsorbed on the surface of porous materials, this analysis modifies the pressure until equilibrium is reached. Two material characteristics were measured using the equipment described within Section 2.4.2: BET surface, which indicates the modifications on the overall material's surface after doping, and the total surface of the micropores. As stated before, one drawback of using carbonic materials for H_2 storage is the low number of micropores and thus the inability to establish strong physical bonds between H_2 molecules and pore walls. BET surface was determined using physical adsorption. Physisorbed molecules are fairly free to move around the surface of as ample. As more gas molecules are introduced within the system, the adsorbate molecules tend to form a thin layer that covers the entire adsorbent surface. Based on well-known BET theory, one can estimate the number of molecules necessary to cover the adsorbent surface with a monolayer of adsorbed molecules. Multiplying that number with the cross-sectional area of an adsorbate molecule yields the sample's surface area. Continued addition of gas molecules beyond monolayer formation leads to the gradual stacking of multiple layers on top of each other. Computational methods, such as the one developed by Barret, Joyner and Halenda (BJH), allow the computation of pore sizes from equilibrium gas pressures. One can therefore generate experimental curves linking adsorbed gas volumes with relative saturation pressures at equilibrium and convert them to cumulative or differential pore-size distributions [13].

Figures 3 and 4 show the BET plots for the initial and doped materials (MW-CNTs and p-$C_6H_5NH_2$). The software Autosorb-1 AS1, used in the above-described equipment,

automatically calculated the samples' surface areas and micropore areas using the multipoint BET method for surface-area calculation and the Langmuir isotherm for the surface area of the micropores calculus.

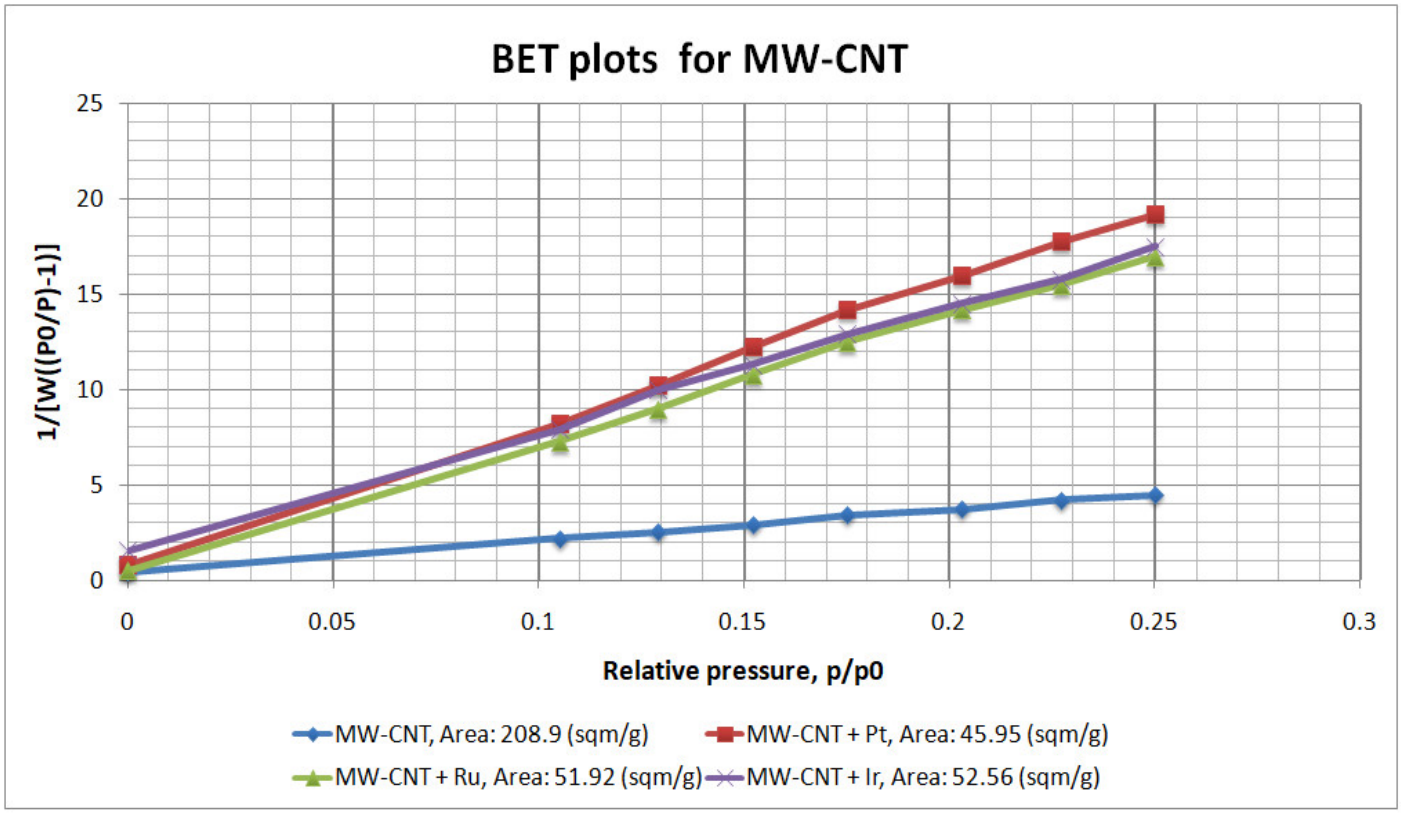

Figure 3. BET plots for the doped and undoped MW-CNTs.

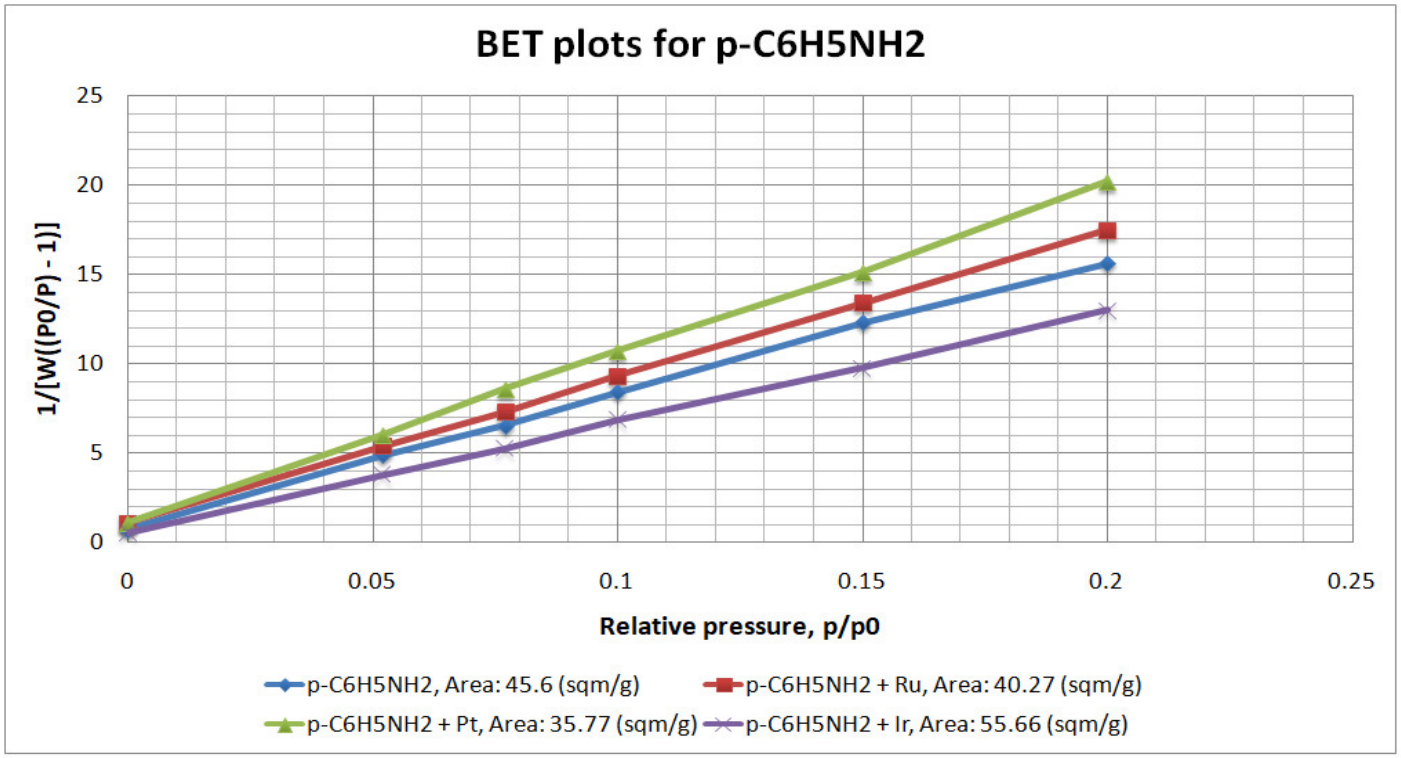

Figure 4. BET plots for the doped and undoped p-$C_6H_5NH_2$.

The obtained numerical values are presented in Table 1, which also contains the percentages of increase/decrease and the ratios between BET and micropore surfaces.

Table 1. Numerical values for BET and micropore surfaces.

	S_BET	S_MICRO	BET Surface Variation	Micropore Surface Variation	S_MICRO/S_BET
	[m²/g]	[m²/g]	%	%	%
MW-CNT	208.9	5.0			2.4
MW-CNT + Pt	46.0	12.0	454.6	240.0	26.0
MW-CNT + Ir	52.6	51.4	397.5	1032.1	97.8
MW-CNT + Ru	51.9	48.6	402.3	975.3	93.5
p-$C_6H_5NH_2$	46.0	4.1			8.9
p-$C_6H_5NH_2$ + Pt	35.8	11.0	77.8	267.3	30.6
p-$C_6H_5NH_2$ + Ir	55.7	53.4	121.0	1302.0	95.9
p-$C_6H_5NH_2$ + Ru	40.0	38.0	87.0	926.8	95.0
		Initial value			
		Increase			
		Decrease			

As can be observed, the BET surfaces of all the materials decreased after doping, except for p-$C_6H_5NH_2$ + Ir, the surface of which increased by 21%. This increase may be a consequence of a secondary release of gases resulting from the chemical reaction between the substrate (p-$C_6H_5NH_2$) and $IrCl_3$ during the doping procedure, thus forming the additional porosity.

In addition, a noticeable result was that, even though, initially, the BET surface of the MW-CNT was 4–5 times bigger than that of the p-$C_6H_5NH_2$ (208.9 vs. 46 m²/g), after the doping procedure, the values became comparable.

The increases in micropore surfaces and also the ratio of micropores to BET surfaces in the cases of Ir and Ru were impressive compared to Pt, but the H_2-adsorption capacities of the carbonic materials doped with these metals proved to be lower than those of the Pt-doped ones.

3.3. H_2-Adsorption-Capacity Assessment

As stated before, ref. [2] demonstrated that nanostructured carbonic materials are not suitable for H_2 storage unless their inner structures are drastically modified. So, after doping them with Pt, Ir and Ru and modifying their structures, the adsorption capacity for H_2 storage was measured by the means described in Section 2.5.

The main aspect to be considered is that the working temperature was kept at 293 ± 5 K, so that only the gas pressure influenced the adsorption capacity. Experiments were carried out at three different pressures: 10, 20 and 30 bar, considered as moderate since a regular LPG tank is able to retain up to 11 bar of gas and, in this particular case, the gas was stored in solid materials, so the danger that usually occurs in the case of regular gas stored at 30 bar was diminished.

The method of measurement consisted of the following steps: ~1 g of material milled to 5 μm was put in the measurement cell at surrounding pressure. An initial gas pressure was set, and the equipment started to feed the testing cell until Δp = set p and the working p was <1 bar. After that, the pressure was kept constant until equilibrium was reached and the gas was stored within the material. The equipment kept feeding the cell with gas until no pressure difference was measured. After that, the pressure was slowly released and the difference between the inserted and released gas volumes was read and transformed into wt.%

Figures 5–7 show the variations between the Pt-, Ir- and Ru-doped MW-CNTs at the set pressures (10, 20 and 30 bar).

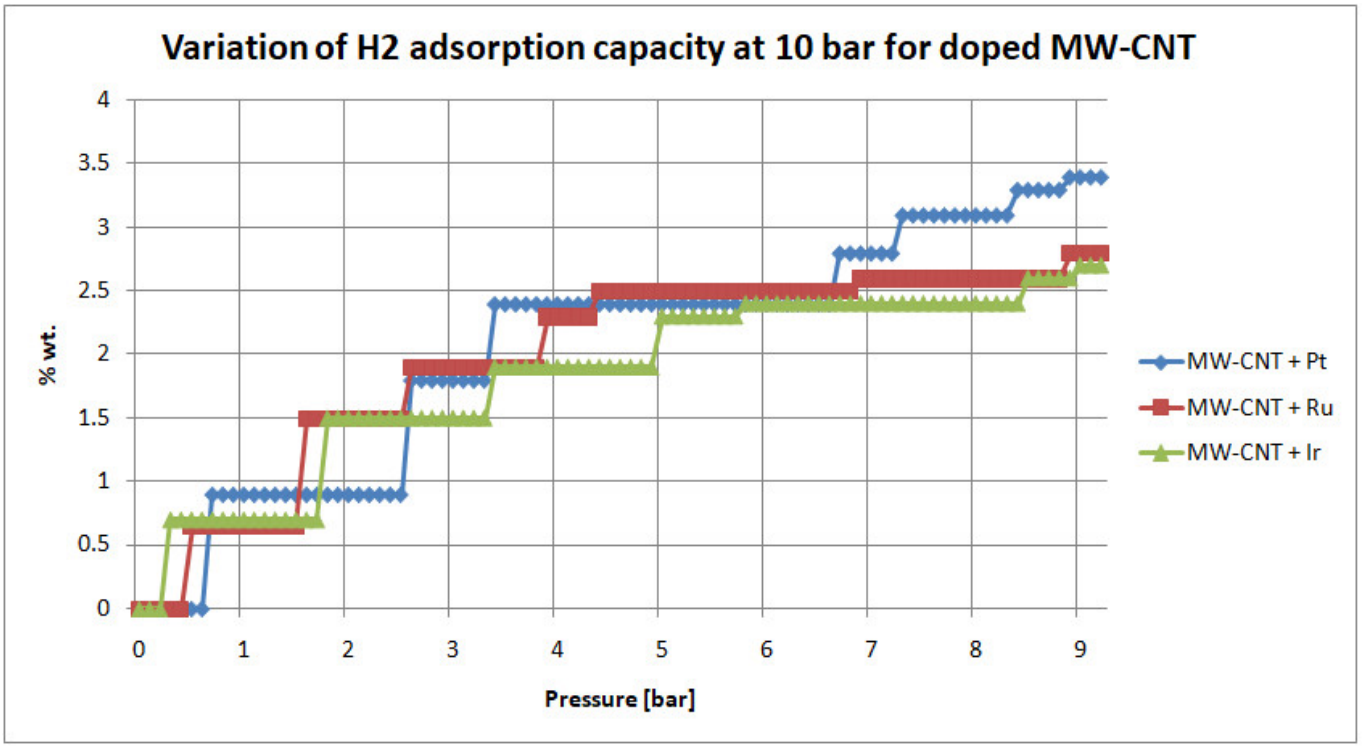

Figure 5. Metal-doped MW-NT H_2-adsorption-capacity determination at 10 bar.

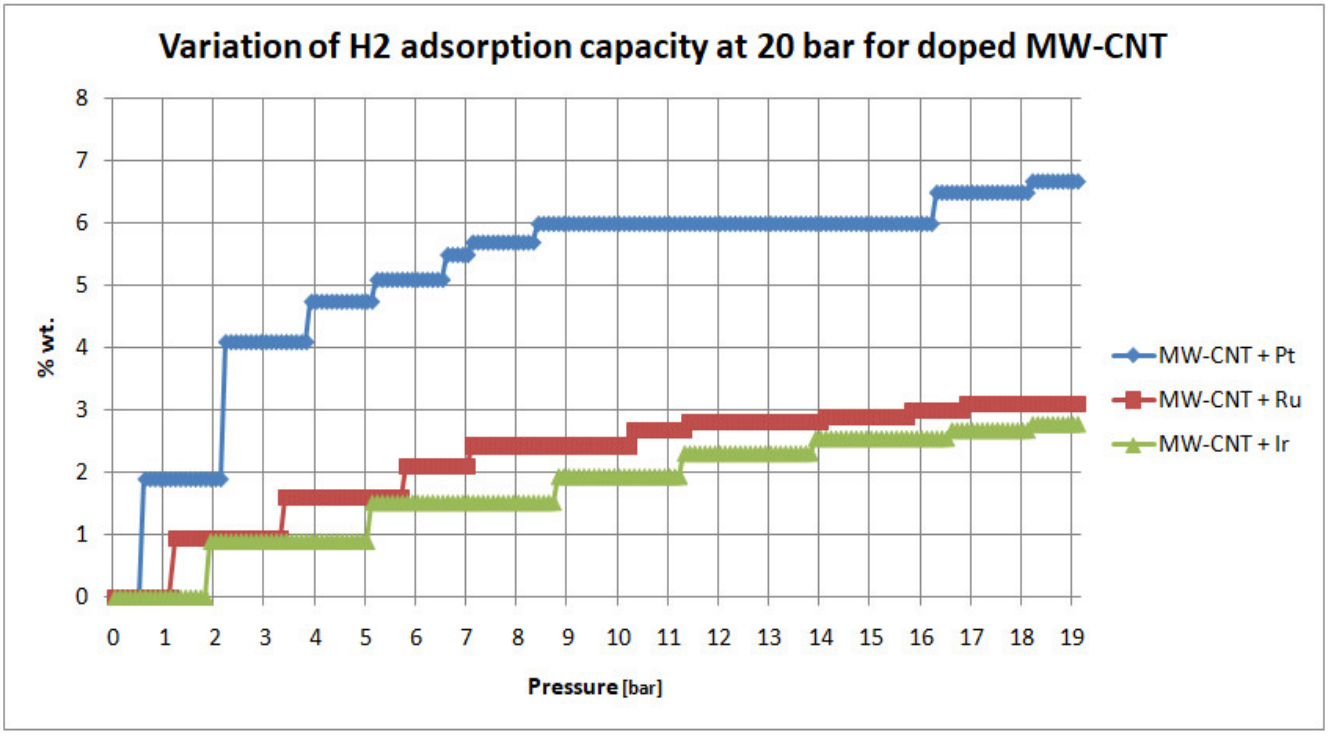

Figure 6. Metal-doped MW-NT H_2-adsorption-capacity determination at 20 bar.

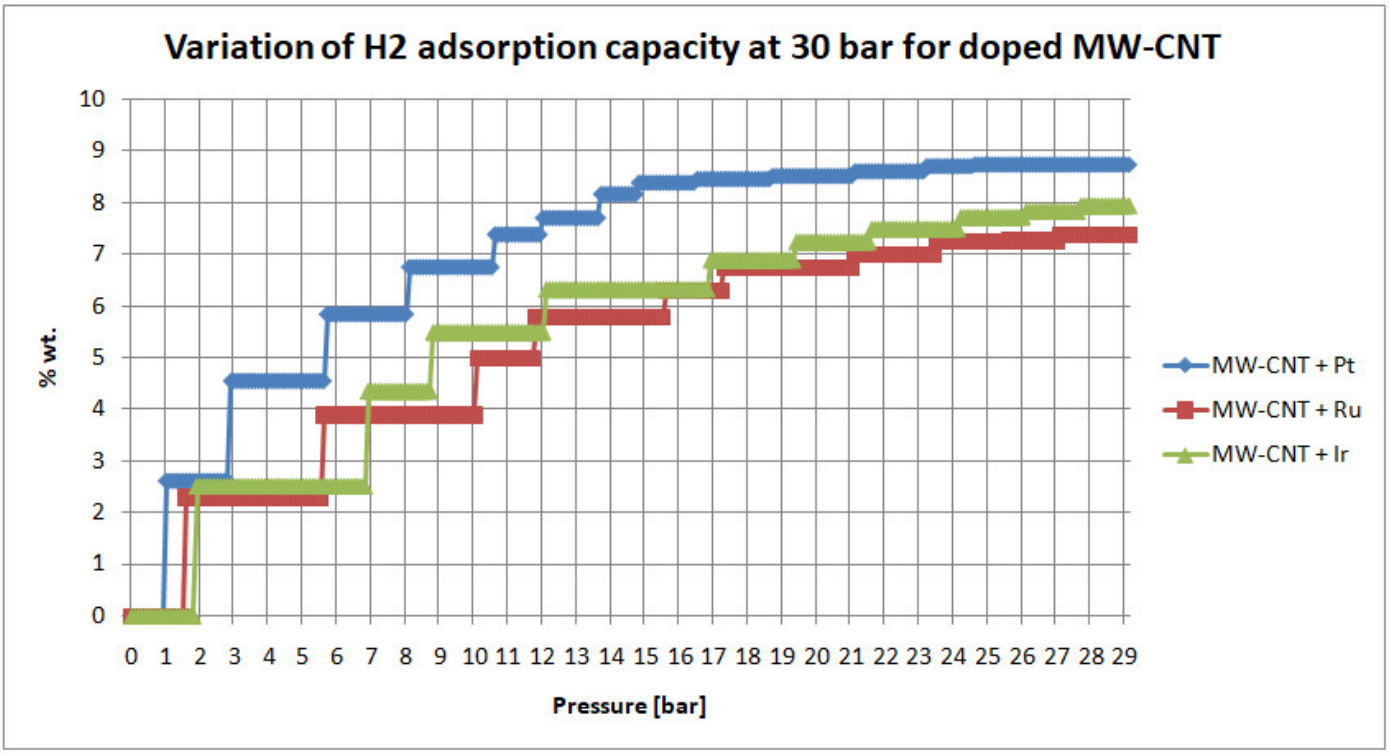

Figure 7. Metal-doped MW-NT H_2-adsorption-capacity determination at 30 bar.

As expected, H_2 adsorption capacity increased as the set pressure increased. Nevertheless, the results showed an interesting aspect, namely, whatever the pressure, the Pt-doped MW-CNTs had higher H_2-adsorption capacities than the Ir- and Ru-doped MW-CNTs, regardless of the less impressive results obtained for the BET measurements. As stated in Section 1, the performance of the Pt-doped material is a direct consequence of Pt reactiveness. Increased electronegativity and electron affinity grant superior characteristics in terms of H_2-adsorption capacity.

Thus, in the case of Pt-doped MW-CNTs, at 10 bar, the materials adsorbed 3.4 wt.%, the Ir-doped materials adsorbed 2.71 wt.% and the Ru-doped materials adsorbed 2.73 wt.%. At 20 bar, the tendencies were the same: the Pt-doped materials adsorbed 6.68 wt.%, the Ir-doped materials adsorbed 2.78 wt.% and the Ru-doped materials adsorbed 4.97 wt.%.At 30 bar, the Pt-doped materials adsorbed 8.73 wt.%, the Ir-doped materials adsorbed 7.95 wt.% and the Ru-doped materials adsorbed 7.38 wt.%.

In the case of the metal doping of the MW-CNTs, the Ru-doped materials seemed to break through, since, at all measured pressures, their performance was similar to that of the Pt-doped materials, but, in term of prices, Ru is almost eight times cheaper than Pt.

The same experiments were performed on metal-doped p-$C_6H_5NH_2$, and the results are shown in Figures 8–10.

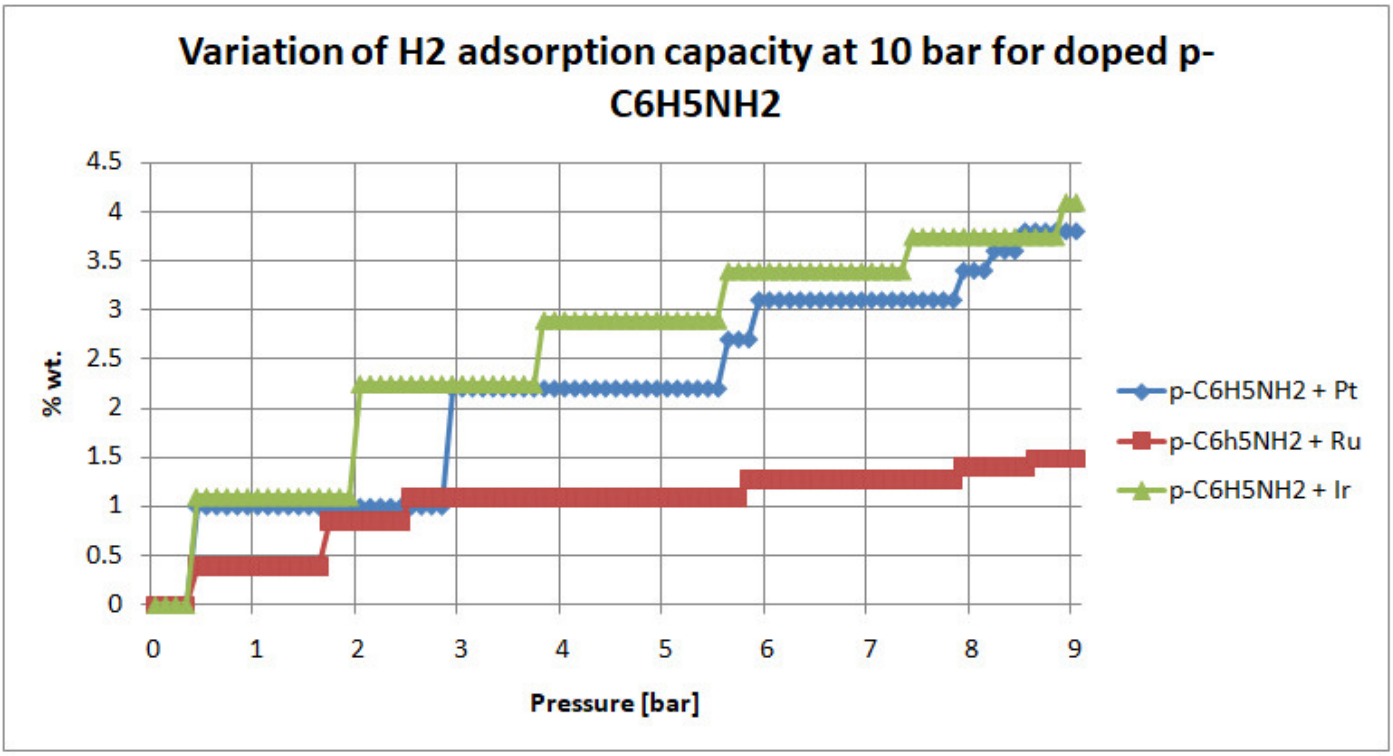

Figure 8. Metal-doped p-$C_6H_5NH_2$ H_2-adsorption-capacity determination at 10 bar.

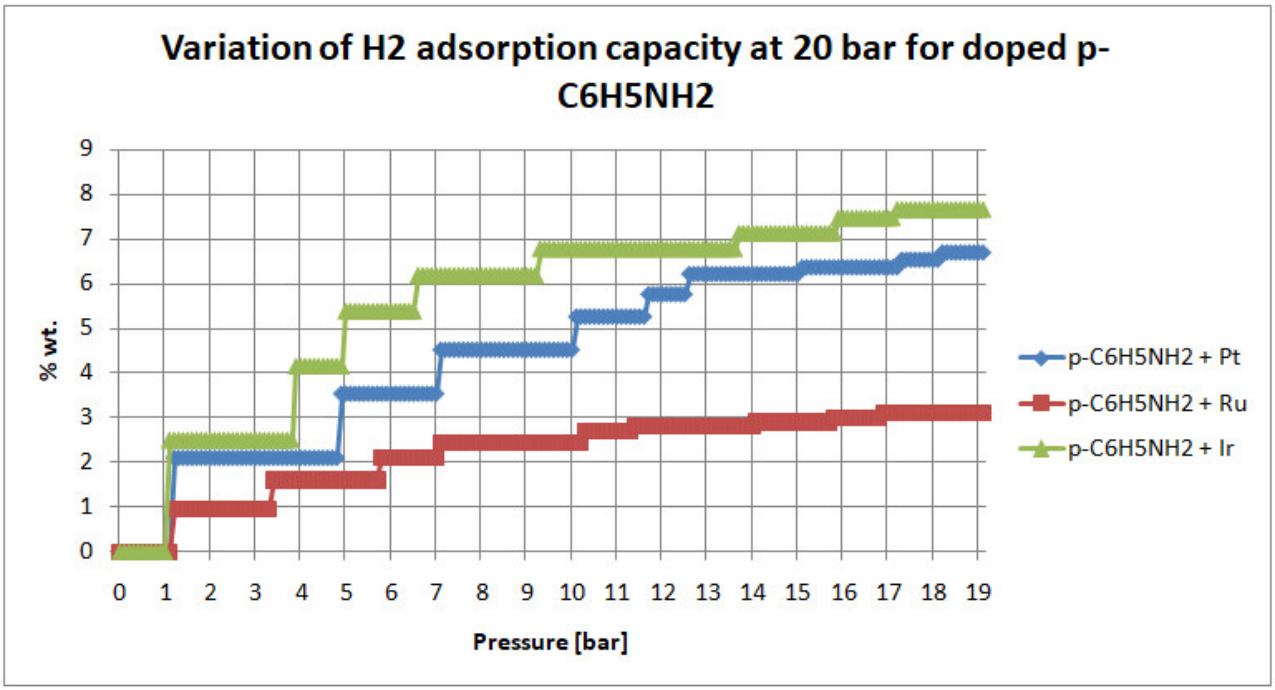

Figure 9. Metal-doped p-$C_6H_5NH_2$ H_2-adsorption-capacity determination at 20 bar.

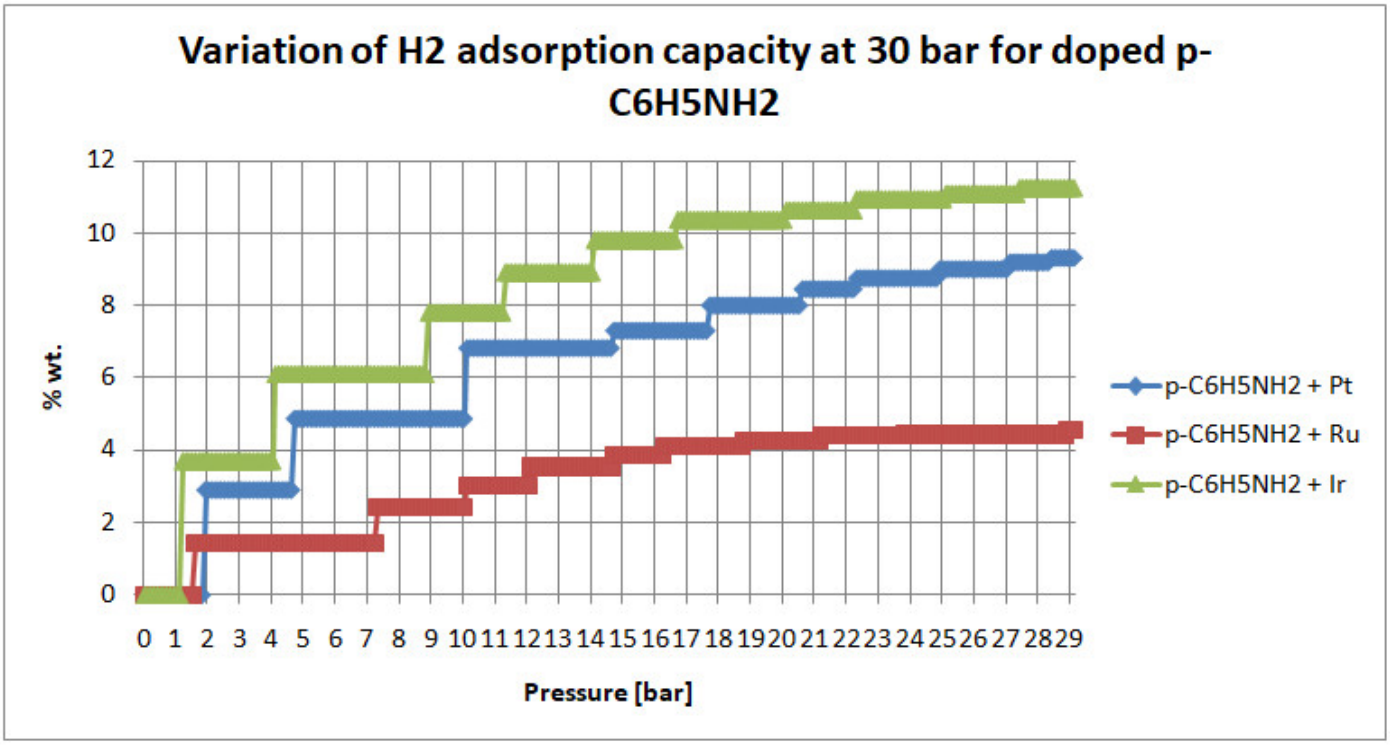

Figure 10. Metal-doped p-$C_6H_5NH_2$ H_2-adsorption-capacity determination at 30 bar.

Broadly speaking, the overall tendency observed in the case of p-$C_6H_5NH_2$ was similar to that observed for the MW-CNTs, but the obtained values were lower. This shows that carbon nanotubes are better for H_2 adsorption than polyaniline, mainly due to their tubular structure and quasi-regulate shape, which allows, on the one hand, large BET and micropore surfaces and, on the other hand, a better anchorage for the metals within their structures.

Thus, in the case of Pt-doped p-$C_6H_5NH_2$, at 10 bar, the material adsorbed 3.73 wt.%, the Ir-doped material adsorbed 4.1 wt.% and the Ru-doped material adsorbed 1.53 wt.% At 20 bar, the tendencies were maintained: the Pt-doped material adsorbed 6.68 wt.%, the Ir-doped material adsorbed 7.65 wt.% and the Ru-doped material adsorbed 3.1 wt.%.At 30 bar, the Pt-doped material adsorbed 9.31 wt.%, the Ir-doped material adsorbed 11.24 wt.% and the Ru-doped material adsorbed 4.53 wt.%. In the case of the p-$C_6H_5NH_2$ substrate, Ir showed the best results, since it allowed higher adsorption capacities to be reached even at low pressures (e.g., 4.1 wt.% at 10 bar).

The shapes of the adsorption curves were due to the method used by the equipment when measuring adsorption capacity at a given pressure. Thus, the materials were put in a tightly closed recipient and pressurized hydrogen was fed in. The temperature was 293 ± 5 K, so that only the pressure influenced the adsorption capacities of the tested materials. The pressure was kept constant until equilibrium was reached. Then, a further increase in the pressure was initiated by the equipment, and so on, until the final pressure and equilibrium were reached. It is widely known that for gas molecules to "travel" within substrate materials they need some time. This is exactly what the equipment ensured: it fed gas at a set pressure, then waited until equilibrium was reached.

Table 2 shows the results obtained in this study compared with the ones reported in the literature.

Table 2. Comparison of the obtained results and those reported in the literature.

	Min.	Material	Temp.	Pressure	Max.	Material	Temp.	Pressure
Paper	**wt.%**		**K**	**bar**	**wt.%**		**K**	**bar**
Current	1.53	p-$C_6H_5NH_2$ + Ru	293	10	11.42	p-$C_6H_5NH_2$ + Ir	293	30
[14]	0.003	Ni MCN 41	77	10	0.0012	Ti MCN 41	77	10
[15]	2.26	$C_6H_6Be(C_4B_2H_6Be)$	N/A	N/A	7.54	$C_6H_6Ti(C_4B_2H_6Ca)$	N/A	N/A
[16]	N/A	N/A	N/A	N/A	14.29	BGDY 4Li	100	1

Table 2 clearly shows that the presented research achieved some promising results with the working parameters of a temperature of 293 K and a pressure of 30 bar.

4. Conclusions

Nanostructured carbonic materials can be used as H_2-storage materials after metal doping and structural modification. Thus, reactive metals, such as Pt, Ir and Ru, may allow the use of carbonic nanostructured materials for adsorption of up to 11 wt.% at room temperature and 30 bar.

Even though Pt is known as a catalyst in chemical reactions involving hydrogen and is the most reactive of all the metals used in this study, Ru seems to be a better choice when considering the financial aspect, allowing performances close to Pt in the case of the MW-CNT substrate, while Ir seems to be the better choice in the case of p-$C_6H_5NH_2$ as a substrate.

The H_2-adsorption capacities of all the materials increased as the pressure increased, and in terms of substrate performance, they each have their own advantages. Thus, MW-CNTs showed superior characteristics due to their tubular structure and quasi-regulate shape when doped with Ru. The main influencing factor may be considered to have been the substrate's sp^3 hybridization for the MW-CNTs vs. the sp^2 hybridization for p-$C_6H_5NH_2$, which allowed an easier transfer of H_2 to the substrate, even though the doping metal was the same. In the case of p-$C_6H_5NH_2$ doped with Ir, the adsorption capacity increased mainly due to the increase in the BET and micropore surfaces after doping.

Micropores play an essential role in carbon nanostructured materials due to the attractive potential of the pore walls.

It has been established that, at 20 bar and room temperature, the target set by the US Department of Energy of 4.5 wt.% H_2 adsorption within a carrier material [7] was reached with the metal-doped nanostructured carbonic materials, thus showing promise for application within the automotive sector.

Polyaniline's initial BET surface may not have been as impressive as that of the MW-CNTs but, after the doping procedure, the values became comparable.

Author Contributions: Conceptualization: G.A.R. and R.M.; validation: R.M. and M.I.; investigation: R.M., G.A.R. and M.I.; data acquisition: M.I.; writing—original draft preparation: R.M.; writing—review and editing: R.M. All authors have read and agreed to the published version of the manuscript.

Funding: The work was performed under contracts no. 46N/2019 and 25PFE/2021 between National Institute for R&D in Electrical Engineering ICPE-CA and the Romanian Ministry of Research, Innovation and Digitization and the contract no. 221/2021 between National Institute for R&D in Electrical Engineering ICPE-CA and the Executive Unit for the Financing of Higher Education, Research, Development and Innovation (UEFISCDI).

Acknowledgments: The authors would like to acknowledge financial support from the management of INCDT COMOTI.

Conflicts of Interest: The authors declare no conflicts of interest. The funders had no role in the design of the study; in the collection, analyses, or interpretation of data; in the writing of the manuscript, or in the decision to publish the results.

References

1. Liu, C.; Chen, Y.; Wu, C.Z.; Xu, S.T.; Cheng, H.M. Hydrogen storage in carbon nanotubes revisited. *Carbon* **2010**, *48*, 452–455.
2. Dillon, A.C.; Nelson, B.P.; Zhao, Y.; Kim, Y.-H.; Tracy, C.E.; Zhang, S.B. Importance of Turning to Renewable Energy Resources with Hydrogen as a Promising Candidate and on-board Storage a Critical Barrier.*MRS Online Proc. Libr.* **2006**, *895*, 503.
3. Ulrich, J. Tiny Tubes: Hydrogen Storage inside Single-Walled Nanotubes. Available online: http://materialsviews.com/tiny-tubes-hydrogen-storage-inside-single-walled-nanotubes/ (accessed on 11June 2013).
4. Corgnale, C.; Hardy, B.; Chahine, R.; Zacharia, R.; Cossement, D. Hydrogen storage in a two-liter adsorbent prototype tank for fuel cell driven vehicles. *Appl. Energy* **2019**, *250*, 333–343.
5. MacDiarmid, A.G. Conducting polymers as potential new materials for hydrogen storage. In Proceedings of the IPHE International Hydrogen Storage Technology Conference, Lucca, Italy, 19–22 June 2005.
6. Gao, L.; Yoo, E.; Nakamura, J.; Zhang, W.; Chua, H.T. Hydrogen storage in Pd-Ni doped defective carbon nanotubes trough the formation of CHx (x+1, 2). *Carbon* **2010**, *48*, 3250–3255. https://doi.org/10.1016/j.carbon.2010.05.015.
7. Available online: https://www.energy.gov/eere/fuelcells/hydrogen-storage (accessed on 23 November 2021).
8. Orinakova, R.; Orinak, A. Recent applications of carbon nanotubes in hydrogen production and storage. *Fuel* **2011**, *90*, 3123–3140.
9. Qiu, B.; Wang, J.; Li, Z.; Wang, X.; Li, X. Influence of Acidity and Oxidant Concentration on the Nanostructures and Electrochemical Performance of Polyaniline during Fast Microwave-Assisted Chemical Polymerization. *Polymers* **2020**, *12*, 310. https://doi.org/10.3390/polym12020310.
10. Bláha, M.; Marek, F.; Morávková, Z.; Svoboda, J.; Brus, J.; Dybal, J.; Prokeš, J.; Varga, M.; Stejskal, J. Role of p-Benzoquinone in the Synthesis of a Conducting Polymer, Polyaniline. *ACS Omega* **2019**, *4*, 7128–7139.
11. Rimbu, G.A.; Jackson, C.L.; Scott, K. Platinum/carbon/polyaniline based nanocomposites as catalysts for fuel cell technology. *J. Optoelectron. Adv. Mater.* **2006**, *8*, 611–616.
12. Available online: http://www.timesnano.com/en/view.php?prt=3,29,50,83 (accessed on 22 November 2020).
13. Babiarz, A.; Klamka, J.; Czornik, A.; Niezabitowski, M. *Theory and Applications of Non-Integer Order Systems*; Springer: Berlin/Heidelberg, Germany, 2017; ISSN 1876-1100.
14. Yaqoob, A.A.; Ibrahim, M.N.M.; Ahmad, A.; Reddy, A.V.B. Toxicology and Environmental Application of Carbon Nanocomposite. In *Environmental Remediation through Carbon Based Nano Composites*; Green Energy and Technology; Springer: Singapore, 2020.
15. Carraro, P.M.; Spang, K.; Oliva, M.I.; Eimer, G.A. Comparative study of hydrogen storage on metal doped mesoporous materials. *Chem. Phys. Lett.* **2018**, *701*, 93–97.
16. Tavhare, P.; Titus, E.; Chaudhari, A. Hydrogen adsorption on metal-functionalized benzene and B-substituted benzene. *Int. J. Energy Res.* **2021**, *45*, 18810–18826. https://doi.org/10.1002/er.6986.
17. Hussain, T.; Mortazavi, B.; Bae, H.; Rabczuk, T.; Lee, H.; Karton, A. Enhancement in hydrogen storage capacities of light metal functionalized Boron-Graphdiyne nanosheets. *Carbon* **2019**, *147*, 199–205.
18. Divya, P.; Ramaprabhu, S. Hydrogen storage in platinum decorated hydrogen exfoliated graphene sheets by spillover mechanism. *Phys Chem.-Chem. Phys.* **2014**, *16*, 26725–26729.
19. Wang, L.; Yang, R.T. Hydrogen storage properties of carbons doped with Ruthenium Platinum and Nickel nanoparticles. *J. Phys. Chem. C* **2008**, *112*, 12486–12494.
20. Hirscher, M.; Yartys, V.A.; Baricco, M.; von Colbe, J.B.; Blanchard, D.; Bowman, R.C., Jr.; Broom, D.P.; Buckley, C.E.; Chang, F.; Chen, P.; et al. Materials for Hydrogen-based energy storage-past, recent progress and future outlook. *J. Alloy. Compd.* **2020**, *827*, 153548.